Class I HDAC Inhibitor Rescues Synaptic Damage and Neuron Loss in APP-Transfected Cells and APP/Ps1 Mice through the GRIP1/AMPA Pathway

Ying Han
Dalian Medical University
Le Chen
Dalian Medical University
Jingyun Liu (ljy8787@163.com)
Dalian Medical University https://orcid.org/0000-0001-5189-505X
Chunyang Wang
Dalian Medical University
Yu Guo
Dalian Medical University
Xuebin Yu
Dalian Medical University
Chenghong Zhang
Dalian Medical University
Haiying Chu
Dalian Medical University
Haiying Ma
Dalian Medical University https://orcid.org/0000-0002-1314-7816

Research Article

Keywords: Alzheimer's disease, HDAC inhibitor, β-amyloid, synapse, AMPA receptor

Posted Date: December 3rd, 2021

DOI: https://doi.org/10.21203/rs.3.rs-1119498/v1

Abstract

As a neurodegenerative disease, Alzheimer's disease (AD) seriously affects the health of older people. It is now known that changes in synapses occur first in the course of disease, perhaps even before the formation of Aβ plaques. Histone deacetylase (HDAC) can mediate the damage of Aβ oligomers to dendritic spines. Therefore, we examined the relationship between HDAC activity and synaptic defects by using an HDACI, BG45 in Human neuroblastoma SH-SY5Y cell line with stable overexpression of Swedish mutant APP (APPsw) and in APP/Ps1 transgenic mice during this study. The cells were treated with 15μM BG45 and the APP/Ps1 mice 30mg/kg BG45. We detected the level of synapse-related proteins, HDACs, tau phosphorylation and AMPA receptors by western bloting and immunohistochemistry. We also measured the expression of cytoskeletal proteins in the cell model. The mRNA level of GRIK2, SCN3B, SYNPR, Grm2, Grid2IP, GRIP1,GRIP2 were. to explore the effects of HDACi on regulating the synaptic proteins and AMPA receptors. Our studies demonstrated that the expression of HDAC1、HDAC2 and HDAC3 was increased, which was accompanied by the downregulation of the synapse-related proteins synaptophysin (SYP), postsynaptic dendritic protein (PSD-95) and spinophilin as early as 24 h after transfection with APPsw gene. BG45 upregulated the expression of synapse-related proteins and repaired cytoskeletal damage. *In vivo*, BG45 alleviated the apoptotic loss of hippocampal neurons, upregulated synapse-related proteins, reduced Aβ deposition and phosphorylation of tau and increased the level of the synapse-related genes GRIK2, SCN3B, SYNPR, Grm2, and Grid2IP. BG45 increased the expression of the AMPA receptor subunits GluA1, GluA2 and GluA3 on APPsw-transfected cells and increased GRIP1 and GRIP2 expression and AMPA receptor phosphorylation *in vivo*. These results suggest that HDACs are involved in the early process of synaptic defects of AD and that BG45 may rescue synaptic damage and loss of hippocampal neurons by specifically inhibiting HDAC1、HDAC2 and HDAC3, thereby modulating AMPA receptor transduction, increasing synapse-related gene expression and finally improving excitatory synapses. BG45 may be considered as a potential drug for the treatment of early AD for further study.

1. Introduction

Alzheimer's disease (AD) is a degenerative neurological disease with progressive cognitive dysfunction that is sufficient to disrupt daily life. With the increasing prevalence of AD, the need for early diagnosis and treatment is even more urgent. The pathogenesis of AD is complex and diverse, and the etiology has not been fully clarified thus far. The pathogenesis of AD has been found to be closely related to a variety of factors, including genetic, immune, and environmental factors, et al[1]. For many years, research has focused on the β-Amyloid (Aβ) cascade hypothesis, which suggests that AD pathogenesis starts with the production of by the abnormal cutting of amyloid precursor protein (APP) by β- and γ-secretase[2]. When the Aβ monomer is overproduced, it is easily misfolded and converted into dimers or polymers after structural transformation[2]. This kind of material is called an Aβ oligomer. The Aβ oligomer is the most neurotoxic form of Aβ and exists as an intermediate in the polymerization of Aβ[3]. Overproduction of Aβ will not only exacerbate the aggregation process of Aβ but also lead to the formation of plaques[4]. The increase in soluble Aβ changes the activity of each kinase, triggers the hyperphosphorylation of tau

protein, and leads to the oligomerization of microtubule-associated tau protein, which destabilizes microtubules and causes them to disintegrate into filaments and finally, after further condensation, form insoluble neurofibrillary tangles (NFTs)[5]. Intracellular and extracellular Aβ can induce neurotoxicity, which leads to neuronal damage and death and causes synaptic damage[6]. Dysregulation of synaptic plasticity-related mechanisms leads to synaptic dysfunction, generation of senile plaques (SPs) and NFTs causes abnormal synaptic communication, and synaptic damage can cause further neuronal damage and death[7].

However, most of the drugs targeting Aβ have failed in AD drug experimental studies, e.g., Solanezumab[8]. It is reported that Aβ is present in and starts to affect the brain 10 to 15 years before symptoms appear[9]. The failure of previous drug experiments might be due to late intervention. Researchers found that impairment of synaptic function appeared before the emergence of Aβ oligomers, and synaptic impairment is likely to be an earlier event in AD[10]. Researchers have used optogenetics to restore the density of dendritic spines and increase synaptic plasticity to ameliorate early memory impairment in AD[11]. However, this method still involves invasive technology. In view of the above results, we considered whether it is possible to find targeted drugs that rescue synaptic damage and neuron loss in the earlier stages of AD and effectively prevent and delay the occurrence of AD.

It is known that the occurrence and development of AD may result from the interaction of multiple factors, such as aging, genetic mutations, metabolic and nutritional disorders, obesity and inflammation, that may induce epigenetic changes. The modification of gene expression includes DNA methylation and histone acetylation. In studies of the acetylation level of histones in APP/Ps1 transgenic mice, it has been proposed that epigenetic mechanisms are related to the changes in synaptic function and memory associated with AD[12]. In addition, it has been found that histone deacetylase (HDAC) activity is increased in an AD mouse model. HDACs can mediate Aβ oligomerization to induce dendritic spine injury, while histone deacetylase inhibitors (HDACIs) can improve this phenomenon[13]. HDACs regulate the chromosome structure and gene transcription together with histone acetyltransferases (HATs). HATs acetylate histones, facilitate DNA and histone depolymerization, and relax nucleosome structure, enabling transcription factors to interact with specific DNA sites to activate gene transcription; HDACs deacetylate histones and tightly bind DNA with a negative charge, causing to become supercoiled and inhibiting gene transcription. HDACs are classified into the following three types according to whether it is homologous to yeast: Class I (HDAC1, 2, 3, and 8) regulates the acetylation of histones; Class (HDAC4, 5, 6, 7, 9, and 10) regulates the acetylation of histones and non-histone proteins; Class is Nicotinamide adenine dinucleotide (NAD) dependent deacetylase, associated with cellular aging and regulation of energy metabolism. In the hippocampus of aged mice, the overexpression of HDAC2 affects the decrease in dendritic spine density, and has a negative correlation with memory recognition ability[14], indicating that synaptic plasticity can also be negatively regulated by HDAC2.

Some studies have pointed out that class I HDACIs can promote gene transcription and the formation of new synapses[15]. Therefore, it is possible that the study of drugs targeting members of the HDAC family

may become a new direction in AD research. Specific inhibition of HDAC3 has been shown to decrease the deposition of $A\beta_{1-42}$ and the phosphorylation of tau protein and increase the BDNF gene expression in the 3xTg-AD mouse model[16]. Some researchers have pointed out that targeted inhibition of class HDACs can alter or even restore memory impairment in transgenic mice by testing the behavioral assay of the APP/PS1 mice injected the systemic histone deacetylase inhibitor (HDACi)[17].

In this study, SH-SY5Y cells transfected with the APP Swedish mutant gene and APP/Ps1 transgenic mice were used as cellular and animal models of AD and were treated with a class I HDAC inhibitor (BG45) to explore the early synaptic damage of AD, the protective effect and mechanism of BG45 against the damage of AD to provide new ideas for clinical intervention and treatment of AD.

2. Materials And Methods

2.1 Cell Culture, Differentiation, Transfection

The Human neuroblastoma SH-SY5Y cell line was cultured in DMEM media (Gibco, USA) supplemented with 10% fetal bovine serum (FBS) (BI, Israel), and 1% penicillin/streptomycin in a 5% CO2 humidified atmosphere at 37°C. Cell differentiation was induced by treatment with 10 μM all-trans retinoic acid (RA) for 7 days. SH-SY5Y Cells were transfected with recombinant plasmid *p-EGFP-N2-APPsw* (APPsw) for establishing an Alzheimer's disease cell model. Empty plasmid *p-EGFP-N2* (GFP) transfected SH-SY5Y Cells for control group, referring to the cells expressing empty cassette. Cell transfection used Effectene Transfection Reagent (QIAGEN, Germany), and cells were subsequently selected by puromycin resistance.

2.2 Drug Preparation

BG45, as a class histone deacetylase inhibitor, is easily dissolved into Dimethyl sulfoxide(DMSO). BG45 was first prepared into 1mg/ml storage solution with DMSO, and then diluted with aqueous solution (normal saline) at 1:1000 for use.

2.3 CCK-8 Assay

Cell viability was measured in 96-well plates with CCK-8 assays. Three times gradients (24h, 36h, 48h) and six concentration gradients (0 μm, 5 μm, 10 μm, 15 μm, 20 μm, 25 μm) were set for each well, and two multiple wells were set for repeated detection. After cells were treated with BG45 or a vehicle for the indicated amount of time, 100 μl of CCK-8 solution was added to the medium, and then cells were incubated at 37°C for 1 h. The absorbance at 450 nm was measured using a microplate reader (Thermo Scientific, USA). Cell viability is estimated by the ratio of the optical density (OD) of the treated group to the control group.

2.4 Animals and Treatment

APP/Ps1 transgenic mice were provided by Nanjing Biomedical Research Institute of Nanjing University. All procedures were approved by the Institutional Animal Care and Use Committee of the Dalian Medical

University in Dalian, China. Twenty male APP/Ps1 transgenic mice were randomly divided into the transgenic group (Tg group) and the BG45-treated groups. The BG45-treated groups included a group with one administration cycle at 2 months of age (Tg+2m BG45 group), a group with one administration cycle at 6 months of age (Tg+6m BG45 group), and a group with two administration cycles at 2 months and 6 months (Tg+(2+6) mBG45 group). Intraperitoneal injection (30 mg/kg BG45[15], 0.2ml each mouse) was applied continuously 12 days for one administration cycle in each BG45-treated group. DMSO diluted with normal saline at the same concentration was used as a vehicle in Tg group. Wild-type mice were used as a control group (Wt group). There were 5 mice in each group. When all mice grew to 6 months of age, the mice were killed by spinal cord dislocation, and hippocampus was harvested.

2.5 Western Blot Assay

After cell lysis on ice, the samples were centrifuged at 12000 g at 4℃ for 15 min. Using a BCA kit (Beyotime Biotechnology, China) to determine the total protein concentration of each sample. Lysates containing equivalent amounts of protein (30 μg) were separated by 10% SDS-PAGE and blotted onto PVDF membranes (Millipore, USA); the membranes were blocked with 5% nonfat milk in Tris buffer at room temperature for 2 h. Western blotting was performed by incubation overnight at 4°C with the following antibodies: rabbit anti-APP (1:1000, Abcam, ab32136), rabbit anti-postsynaptic density protein 95 (PSD-95, 1:1000, Abcam, ab18258), rabbit anti-synaptophysin (SYP, 1:1000, Abcam, ab32127), rabbit anti-spinophilin (1:1000, Cell Signaling Technology, 14136), rabbit tau (1:1000, Cell Signaling Technology, 46687), rabbit anti-p-tau (1:1000, Cell Signaling Technology, 20194), rabbit anti-HDAC1, rabbit anti-HDAC2, and rabbit anti-HDAC3 (1:1000, Cell Signaling Technology, 65816), rabbit anti-p-GluR2 (Ser880) (1:1000, Abbkine, ABP54637), rabbit anti-GluA2/3/4 (1:1000, Cell Signaling Technology,2460S), mouse anti-GAPDH (1:5000, Proteintech, 60004-1) and rabbit anti-β-actin (1:1000, ABclone, AC026). After three washes with 1×TBST, the membranes were incubated with a secondary antibody at room temperature for 1 h and then washed again as before. Chemiluminescence was performed on the proteins using the Amersham ECL Western Blotting Detection Kit (GE Healthcare Life Sciences). Then the image exposed by ChemiDOC™ XRS+ with Image Lab™ Software (BIO-RAD Laboratories, Inc., Hercules, CA, USA) was collected. The optical density of the target protein band in each sample is compared with its GAPDH/β-actin band.

2.6 Immunohistochemistry

Cells were seeded on 12-well slides (Solarbio, China). Then the cell climbing slices were washed with PBS, fixed with 4% PFA at room temperature for 20 min, washed 3 times with PBS, and permeabilized in a 0.5% Triton X-100 solution for 10 min. Mouse brains were paraformaldehyde fixed, paraffin-embedded, and cut into sections 10 μm thick. After the sections were deparaffinized to complete hydration, sodium citrate buffer was used for antigen retrieval. The cell climbing slices and mouse brains sections were treated as follows. After washing with PBS, nonspecific antibody sites were blocked by incubation with 5% BSA at room temperature for 1 h. The slides were then incubated with one of the following primary antibodies overnight at 4℃, rabbit anti-NeuN (1:200, Abcam, ab177487), rabbit anti-APP (1:200, Abcam, ab32136), rabbit anti-Aβ (1:200, Cell Signaling Technology, 14975), rabbit anti-spinophilin (1:200, Cell Signaling

Technology, 14136), rabbit anti-caspase3 (1:200, Wanlei, WL01992a) and mouse anti-MAP2 (1:200, Abcam, ab5392). After washing with PBS, the samples were incubated with one of the following secondary antibodies at room temperature for 2 h. Alexa Fluor-488 or Alexa Fluor-647 conjugated goat anti-rabbit antibody (1:300, Vector Laboratories, USA). Then the samples were incubated with the nuclear dye DAPI at room temperature for 10 min for immunofluorescence staining.

For Immunohistochemistry, the slides were dropped anti-Rabbit IgG-Biotin antibody produced in goat to the slides for 15 min at room temperature. After washing with PBS, horseradish peroxidase-labeled streptavidin was added to bind biotin. Finally, staining was visualized with DAB treatment and a Hematoxylin counterstain. Five random slides were selected from each group, and five randomly selected visual fields in the hippocampus region from each slide were observed. Integrated optical density(IOD) was calculated using Image-Pro Plus 5.1 software.

2.7 Labeling Cytoskeletal F-Actin

Cells were seeded on 12-well slides (Solarbio, China). The slides were washed with PBS, fixed in a 4% PFA solution, and cleaned three times. Permeate the cells in 0.5% Triton X-100 solution for 5 min. After PBS washing, the cells were labeled with fluorescein phalloidin (1:200, Sigma) for 20 min at room temperature. The cells were stained with DAPI at room temperature for 10 min after cleaned. The cells were viewed using a fluorescence microscope (Olympus, Japan), and the mean optical densities were quantified using Image-Pro Plus 5.1 software.

2.8 Live cell surface immunostaining

To measure cell surface GluA1, GluA2, and GluA3 levels, GFP- and APPsw-transfected cells were treated with the HDACI BG45 (15 μM) or vehicle. After 36 h, live cells were incubated with GluA1, GluA2, or GluA3 antibodies (10 μg/mL in conditioned medium) for 10 min and were then fixed with 4% PFA under nonpermeabilizing conditions for 5 min. Surface-labeled GluA1, GluA2, and GluA3 were detected with Alexa Fluor-647 secondary antibodies. The cells were viewed using a fluorescence microscope (Olympus, Japan), and the mean optical densities were quantified using Image-Pro Plus 5.1 software.

2.9 Reverse transcription PCR (RT-PCR)

The samples were homogenized with Trizol reagent. Chloroform was added to facilitate the isolation of RNA. After standing at room temperature, the mixture was centrifuged into three layers, the transparent supernatant was taken to the EP tube, and isopropanol of the same volume was added to precipitate the RNA. Then, the samples were washed with 75% ethanol for three times, the supernatant was taken, the RNA samples were dried at room temperature, and the RNA concentration and purity were measured after the precipitation was dissolved. The highest purity of RNA was obtained when A260/A280 = 1.8~2.0.

Total RNA was extracted from transfected cells using TRIzol reagent (Takara) and transcribed using a reverse transcription Kit (Applied Biosystems) according to the manufacturer's instructions. Gene expression levels were analyzed relative to the level of the GAPDH gene transcript. The following primers were used for RT-PCR:

APPsw, F: 5’- TCTGAAGTGAATCTGGATGCA-3’;

R: 5’ - GTTCTGCATCTGCTCAAAGA-3’;

GAPDH, F: 5’-TGTGATGGGTGTGAACCACGAGAA-3’;

R: 5’-GAGCCCTTCCACAATGCCAAAGTT-3’.

cDNA samples were mixed with primers and Dream Taq Green PCR Master Mix (Thermo) in a total volume of 50 μl. The thermal cycling conditions used in the protocol were as follows: 5 min at 94°C followed by 35 cycles at 94°C for 1 min, 55°C for 1 min, 72°C for 2.5 min and 72°C for 10 min. The RT-PCR products were analyzed on a 1% agarose gel, and the sizes were as follows: APP, 315 bp; GAPDH, 130 bp.

2.11 Real-time Quantitative PCR (Real-time PCR)

Total RNA was extracted from the hippocampus using TRIzol reagent (Takara) and transcribed using a reverse transcription Kit (Applied Biosystems) according to the manufacturer’s instructions.

SCN3B, F: 5’-ATGTGTCCAGGGAGTTTGAGT-3’

R: 5’-TTCGGCCTTAGAGACCTTTCT-3’

SYNPR, F: 5’-CAGCATTGACATAGCGTTTGC-3’

R: 5’-GGTTGTTTTCGCGGTACTTGT-3’

GRIK2, F: 5’-CAGCGTCGGCTCAAACATAAG-3’

R: 5’-GGTTTCTTTACCTGGCAACCTT-3’

GAPDH, F: 5’-TGTGATGGGTGTGAACCACGAGAA-3’;

R: 5’-GAGCCCTTCCACAATGCCAAAGTT-3’.

Grid2IP, F: 5'-CGGAGCGCCTCTTAGTGTC-3'

R: 5'-GCCGAAACTCTTGTTGCCTTTAT-3'

Grm2, F: 5'-CTTTGTGCGTGCCTCACTCA-3'

R: 5'-TCATAACGGGACTTGTCGCTC-3'

GRIP1, F: 5'-CAGAGGAGCGACAGACAACAT-3'

R: 5'-GGTGGTACGTGTTATGGTGATG-3'

GRIP2, F: 5'-ATGTTGGCGGTGTCACTCAAG-3'

R: 5'-TGCTGCCCTCACGTTTGAT-3'

mRNA samples were mixed with primers and 2x TransStart Top Green qPCR SuperMix (Transgene) in a total volume of 20 µl. The thermal cycling conditions used in the protocol were as follows: 30 sec at 94°C followed by 45 cycles at 94°C for 5 sec, 60°C for 30 sec, and the dissociation step. The calculated quantity of the target gene for each sample was then divided by the average calculated quantity of the housekeeping genes GAPDH corresponding to each sample to give a relative expression of the target gene for each sample. All experiments were performed in duplicate.

2.12 Statistical Analysis

All values are expressed as the mean ± standard deviation (SD). The statistical analyses were completed with one-way analysis of variance (ANOVA) and Student's t-test. Differences were considered significant at $p < 0.05$.

3. Results

3.1 APP, Aβ and p-tau/tau were increased in stably transfected SH-SY5Y cells.

To induce APP expression and Aβ secretion, SH-SY5Y cells were stably transfected with APPsw to produce an in vitro AD model. CCK-8 assays were used to determine the appropriate concentrations of puromycin. Normal SH-SY5Y cells died when the screening time was 5 days and the concentration of puromycin was 4 µg/ml. Transfection efficiency was observed by fluorescence microscopy (Fig. 1A). The cells were selected by puromycin resistance (4 µg/ml). Expression of the APPsw gene in transfected cells was detected by RT-PCR. The results showed that APPsw cells (SH-SY5Y cells transfected with APPsw) expressed the APPsw gene (Fig. 1B). Moreover, the protein expression of APP in both GFP cells (SH-SY5Y cells transfected with *p-EGFP-N2* for the control group) and APPsw cells was determined by Western blotting and immunofluorescence staining. The APPsw cells showed a significant increase in the expression of APP compared to the GFP cells ($p<0.01$, $p<0.01$) (Fig. 1C, D). Immunofluorescence staining was also performed to assess the Aβ level in the GFP and APPsw cells. The APPsw cells also exhibited a higher Aβ level than the GFP cells ($p<0.01$) (Fig. 1F). Furthermore, because tau protein is hyperphosphorylated and abnormally accumulates in axons, dendrites and cell bodies in AD, Western blot analysis was performed to detect tau protein; the results showed that the tau phosphorylation level was strongly increased in the APPsw cells compared to GFP cells ($p<0.05$) (Fig. 1D).

3.2 The expression of PSD-95 in APPsw cells was significantly downregulated at different times.

Changes in PSD-95 expression can partially reflect the degree of synaptic damage. The results showed that the expression of PSD-95 in APPsw cells was significantly downregulated at 36 h (p<0.001) (Fig. 2A, B), so three time points (24 h, 36 h, and 48 h) were selected for the subsequent experiment.

3.3 BG45 increased APPsw cell viability and decreased the expression of class I HDACs (HDAC 1and 2) in APPsw cells.

Based on the changes in PSD-95 protein expression in APPsw cells at different times, the CCK-8 assay was used to determine the optimal time and concentration for BG45 treatment. The results showed that BG45 had no significant effect on GFP cells either at different time or different concentration. While for the APPsw cell, compared with other groups, the viability of the APPsw cells treated with 15 μM BG45 for 36 h was significantly increased (p<0.05) (Fig. 3A).

To reveal the expression of HDACs in APPsw cells at different times and determine the effect of BG45 on HDAC expression, class I HDACs (HDAC1, 2, and 3) were detected in each group at 24 h, 36 h and 48 h (Fig. 3B). The results showed that compared to that in the GFP group, the expression of HDAC1 in the APPsw group was significantly increased at 36 h and 48 h (p<0.05 and p<0.05) (Fig. 3C). The expression of HDAC2 was significantly increased at 24 h and 36 h (p<0.05 and p<0.01) (Fig. 3D). The expression of HDAC3 in the APPsw group was significantly increased at 36 h (p<0.01) (Fig. 3E). The data suggest that the levels of HDAC1、HDAC2 and HDAC3 were upregulated in the APPsw-transfected cells. While with BG45 treatment, the expression of HDAC1、HDAC2 and HDAC3 in BG45-treated APPsw cells was significantly decreased at each time point compared to that in APPsw cells without BG45 treatment (p<0.05, p<0.05, and p<0.05; p<0.01, p<0.01, and p<0.05; p<0.05, p<0.05, and p<0.05) (Fig. 3C, D, E).

3.4 BG45 significantly decreased the expression of the AD-related protein APP in APPsw cells.

When we concluded that the expression of HDAC1 and HDAC2 was decreased by BG45 treatment of APPsw cells for different amounts of time, we further examined

whether the BG45 can affect the expression of APP protein (Fig. 4A). The results showed that compared with that in the GFP group, the expression of APP in the APPsw group was significantly elevated at 24 h, 36 h and 48 h (p<0.05, p<0.01, and p<0.05) (Fig. 4B). However, the expression of APP in the BG45-treated APPsw cells group was significantly decreased compared to that in the APPse cells without BG45 treatment (p<0.05, p<0.05, and p<0.05) (Fig. 4B).

3.5 BG45 significantly increased the expression of SYP, PSD-95, spinophilin and F-actin.

Next, we investigated whether BG45 affects the expression of the synapse-related proteins SYP, PSD-95 and spinophilin (Fig. 5A). For APPsw groups without BG45 treatment at different time points, we found that the expression of SYP and PSD-95 were significantly decreased at 36 h and 48 h compared to that at

24h (p<0.05, and p<0.05; p<0.05, and p<0.05) (Fig. 5B, C). The expression of spinophilin at the APPsw group without BG45 treatment was significantly decreased at 24 h, 36 h, and 48 h compared to that in GFP groups (p<0.05, p<0.05, and p<0.05) (Fig. 5D). However, as we predicted, BG45 improved the decreased expression of synapse-related proteins. After BG45 treatment, different time points, BG45-treated cells showed significant increases in the expression of SYP and PSD-95 at 36h compared to APPsw group without BG45 treatment, (p<0.01 and p<0.01) (Fig. 5B&C); the expression of spinophilin was also significantly upregulated at 24h and 36h compared with that in APPsw group without BG45 treatment (p<0.01, and p<0.01) (Fig. 5D). In addition, immunofluorescence staining was used to analyze spinophilin morphologically. The results indicated that compared with that in the GFP control group, the expression of spinophilin in the APPsw group was significantly decreased (p<0.05), while the expression in the BG45-treated APPsw group was significantly higher than that in the APPsw group (p<0.05) (Fig. 5E&G).

Furthermore, F-actin staining using phalloidin revealed that compared with those in the GFP control groups, the number of cell processes was decreased, the length protrusions were decreased, and the expression of F-actin was significantly decreased in the APPsw group(p<0.05). Compared with the APPsw group, the BG45 treatment group exhibited significantly repaired cytoskeletal damage (p<0.05) (Fig. 5F&H).

3.6 BG45 increased the cell surface levels of the AMPA receptor subunits GluA1 and GluA2

Amino-3-hydroxy-5-methyl-4-isoxazolepropionic acid receptors (AMPARs) play a central role in the modulation of excitatory synaptic transmission in the central nervous system (CNS). We investigated the effect of BG45 on AMPA receptor trafficking. Detection of fluorescence on the surface of living cells (Fig. 6A) showed that the expression levels of the AMPA receptor subunits GluA1 (p<0.01), GluA2 (p<0.01) and GluA3 (p<0.01) (Fig. 6B-D) in the APPsw cells were significantly downregulated compared with those in the GFP cells. BG45 significantly increased the APPsw cells' levels of the AMPA subunits GluA1 (p<0.05), GluA2 (p<0.05) and GluA3 (p<0.05) (Fig. 6B-D) compared with those APPsw groups without BG45 treatment.

3.7 BG45 alleviated neuronal loss in the hippocampus in APP/Ps1 transgenic mice

To explore the protective effect of BG45 on hippocampal neurons *in vivo*, immunofluorescence was used to detect the co-expression of caspase-3 and MAP2 in hippocampal neurons of APP/Ps1 mice. The results showed that compared with those in the wild-type group, the hippocampal neurons in the Tg group showed a stronger caspase-3 positive signal. Moreover, MAP2, a neuron marker, exhibited weak co-expression. After HDACI treatment, compared with that in the Tg group, caspase3 expression in the Tg+2m BG45 group and the Tg+(2+6)m BG45 group decreased significantly (p<0.01); however, the expression of MAP2 increased significantly (p<0.01, p<0.05), and the effect in the Tg+(2+6)mBG45 group

was better than that in the Tg+2mBG45 group (p<0.01) (Fig. 7A). The rate of MAP2 positive cells showed that

3.8 BG45 decreased Aβ deposition and the phosphorylation level of tau protein in the hippocampus of APP/Ps1 transgenic mice

Immunohistochemistry was used to detect Aβ deposition in the brains of mice in each experimental group. Plaques were observed in all APP/Ps1 transgenic mice at 6 m, and the plaque number in the Tg group was the highest. Compared with that in the Tg group, the plaque numbers in the HDACI treatment groups decreased significantly (p<0.01, p<0.05, p<0.01), among which the number of plaques in the Tg+2mBG45 group and Tg+(2+6)mBG45 group showed the largest decreases, but there were no significant differences among Tg+2mBG45, Tg+6mBG45 and Tg+(2+6)mBG45 groups (Fig. 8A).

Furthermore, Western blotting was used to detect the phosphorylation level of the tau protein. The results showed that compared with that in the Wt group, the phosphorylation level of the tau protein in the Tg group was increased (p<0.01), but with HDACI treatment, the expression of p-tau/tau in the Tg+2mBG45, Tg+6mBG45 and Tg+(2+6)mBG45 groups decreased significantly (p<0.01, p<0.01, p<0.01). Consistent with the results of the Aβ plaque analysis, there were no significant differences among the three groups (Fig. 8C).

3.9 BG45 inhibited HDAC1 and HDAC2 protein expression in the hippocampal neurons of APP/Ps1 mice

Western blotting was used to detect the effect of BG45 on the expression of HDAC1 and HDAC2 in the hippocampus of APP/Ps1 transgenic mice. The results showed that HDAC1 and HDAC2 were highly expressed in the Tg group. Compared with that in the Tg group, the expression of HDAC1 in the 2mBG45, 6mBG45 and 2+6mBG45 groups was significantly decreased (p<0.05, p<0.05, p<0.01). The expression of HDAC2 in the Tg+2mBG45, Tg+6mBG45 and Tg+(2+6)mG45 groups was significantly lower than that in the Tg group (p<0.01, p<0.01, p<0.01). Among the HDACI treatment groups, the effect in the Tg+(2+6)mBG45 group was significantly larger than those in the Tg+2mBG45 and Tg+6mBG45 groups (p<0.05, p<0.05)(Fig. 9A).

3.10 BG45 increased the expression of synapse-associated proteins in the hippocampal neurons of APP/Ps1 mice

The effect of BG45 on the expression of spinophilin in APP/Ps1 mice was detected by immunohistochemistry to evaluate the morphology of dendritic spines. As shown in Fig. 10A, the expression of spinophilin in the hippocampus of the Wt group was high, while that in the hippocampus of the Tg group was significantly lower than it (p<0.01). With the administration of BG45, the protein expressions of spinophilin in the treatment groups (Tg+2mBG45, Tg+6mBG45, and Tg+(2+6)mBG45) were higher than that in the Tg group (p<0.05, p<0.05, p<0.01). Among the treatment groups, the

expression of spinophilin in the Tg+(2+6)mBG45 group is higher than that in the Tg+2mBG45 group (p<0.05).

Subsequently, Western blotting was used to detect the expression of synapse-related proteins. As shown in Fig. 10B, compared with those in the Tg group, the expression levels of spinophilin, PSD-95 and SYP in the hippocampus of the BG45 groups were increased (p<0.05, p<0.01, p<0.01; p<0.05, p<0.05, p<0.01; p<0.05, p<0.01, p<0.001). Among the three groups, the expression of PSD-95 and SYP in the Tg+(2+6)mBG45 group was significantly higher than those in the Tg+2mBG45 and Tg+6mBG45 groups (p<0.05, p<0.05; p<0.01, p<0.01). The expression of spinophilin in the Tg+(2+6)mBG45 group was significantly higher than that in the Tg+2mBG45 group (p<0.05). However, there was no statistical significance compared with the Tg+6mBG45 group (p>0.05).

3.11 Effects of BG45 on the mRNA levels of synapse-related genes in the hippocampal neurons of APP/Ps1 mice

Real-time PCR was used to detect the mRNA levels of synaptse-related genes (GRIK2, SCN3B, SYNPR, Grm2, and Grid2IP) in the hippocampus of APP/Ps1 transgenic mice treated with BG45 (Fig. 11A-E). The results showed that the mRNA expression levels of GRIK2, SCN3B and SYNPR in the Tg+2mBG45, Tg+6mBG45 and Tg+(2+6)mBG45 groups were significantly higher than those in the Tg group, especially in the Tg+(2+6)mBG45 group, which showed significantly higher mRNA levels than the Tg+2mBG45 and Tg+6mBG45 groups (p<0.01, p<0.01, p<0.01; p<0.01, p<0.05, p<0.01; p<0.001, p<0.01, p<0.01). The mRNA expression levels of the other two genes Grm2 and Grid2IP, were also significantly higher in the Tg+(2+6)m BG45 group than in the other two groups (p<0.01; p<0.05, p<0.05).

3.12 Effects of BG45 on amino-3-hydroxy-5-methyl-4-isoxazolepropionic acid receptors (AMPARs) and related gene levels in the hippocampal neurons of APP/Ps1 mice

Real-time PCR was used to detect the effect of BG45 on the mRNA expression of GRIP1 and GRIP2 in the hippocampus of APP/Ps1 transgenic mice. The results showed that compared with those in the Wt group, the mRNA expression levels of GRIP1 and GRIP2 in the Tg group were significantly decreased (p<0.01; p<0.01). After BG45 treatment, their mRNA expression levels in the Tg+(2+6)mBG45 group were higher than those in the Tg+2mBG45 and Tg+6mBG45 groups (p<0.01, p<0.05; p<0.01, p<0.01)(Fig. 12A, B).

Western blot was used to detect the expression of AMPA receptors (Glu2/3/4) and the phosphorylation level of serine 880 site (S880) on GluR2. As shown in the Fig. 12C-D, compared with the wild-type group, the phosphorylation level of the serine 880 site of GluR2 in the hippocampus of the Tg group were increased (p<0.01). The phosphorylation level in the Tg+6mBG45 group was higher than that in the Tg+2mBG45 and Tg+(2+6)mBG45 groups (p<0.01, p<0.01), but there was no significant difference with the Tg groups (p>0.05). Moreover, the phosphorylation levels in the Tg+2mBG45 and Tg+(2+6)mBG45 groups decreased significantly with the Tg group (p<0.01, p<0.01).

4. Discussion

Memory deficits in patients with AD is one of the most important factors affecting the quality of life. Some studies have found that the targeting of HDACI to class HDACs can improve the contextual memory and spatial memory deficits in the mouse model of AD[17, 18]. These results indicate that targeting class HDACs might be a promising approach for the intervention of AD. APP is a protein that has been widely studied in the field of AD pathology[19, 20]. APPsw-transfected neuron-like cells have robust expression of APP and are a reliable system of producing Aβ *in vitro* that can model the pathological characteristics of AD[21]. SH-SY5Y cell was derived from human neuroblastoma, which could be induced by All-trans retinoic acid (RA) into the neuronal differentiation. In the study, the cells were transfected with a Recombinant Plasmid *p-EGFP-N2-APPsw* for establishing an Alzheimer's disease cell model. The increased expression of APP and Aβ and the increased level of tau phosphorylation indicated that the cell model was successfully constructed and could be used in subsequent *in vitro* experiments. Furthermore, the APP/Ps1 transgenic mouse was used as an animal AD model *in vivo*. We investigated the protective effects of BG45 on APPsw gene-transfected SH-SY5Y cells and APP/Ps1 transgenic mice. In our previous studies, we found that BG45 ameliorated the decrease in synaptic protein expression caused by exogenous Aβ by peripheral administration in cells and animal models[22]. Therefore, to further explore the underlying mechanism of HDACI in improving synaptic plasticity, in this study, we used gene transfection to mediate the production of Aβ by cells themselves to study the effects of HDACI on early AD, and the relationship between the HDACI, synaptic protein, synapse-related genes and receptors.

It has been reported that the expression of HDAC2 is significantly increased in the brains of AD patients and the CK-p25 and 5xFAD transgenic mouse AD models and in *in vitro* AD-related neurotoxicity injury models[23]. Overexpression of HDAC2 causes decreased dendritic spine density, synapse number, synaptic plasticity and memory formation, whereas overexpression of HDAC1 does not produce such effects[24]. In addition, Lentivirus-mediated overexpression of HDAC3 used in the APP/Ps1mice also activated microglia cells, increased the level of Aβ and decreased the spine density[18]. In this study, data showed that the expression of HDAC2, HDAC3 in APPsw cells were higher than in control cells.

To verify the correlation between HDACs and synapse-associated proteins in the AD cell model, we detected the expression of AD-related proteins and synapse-related proteins at 24 h, 36 h, and 48 h. The results showed that APP protein level was high in the APPsw group at 24 h. Moreover, we observed that spinophilin showed a significant decrease at 24 h; further, SYP and PSD-95 levels began to decrease at 36 h, which was consistent with the increase in HDAC1HDAC2 and HDAC3. Kilgore, M., et al. reported that after inhibition of HDAC1, 2, and 3 by RGFP963, the result of contextual fear conditioning test in APP/PS1 mice showed that the inhibitors improved synaptogenesis and memory impairment[17]. While lentivirus-mediated shRNA inhibition of HDAC3 reduced amyloid burden and Aβ levels, and rescued spatial memory impairment in APP/PS1 mice[25]. Therefore, we assumed that, in the study, decreased expression of synapse-related proteins is associated with increased expression of HDACs. As a structural component of the presynaptic membrane and synaptic vesicles, SYP is a representative structural protein

involved in the neurogenic budding reaction, and it is specifically distributed in the presynaptic membrane. It is mainly transported to the terminal ends of axons after neuron cell synthesis. The expression levels of SYP and PSD-95 can be used to assess synaptic distribution and density[26]. We found that BG45 reduced the expression of HDAC1、HDAC2 and HDAC3 either prior to or while these synapse-associated proteins, including PSD-95, SYP and spinophilin, began to be changed significantly by increased APP in APPsw cells.

The number and morphological changes of dendritic spines on hippocampal neurons are considered to be the cellular basis of learning and memory[27]. Spinophilin is a multifunctional protein located on the dendritic spine, and it regulates the membrane and cytoskeleton and plays an important role in the central nervous system. It is closely related to the number and morphology of dendritic spines and the formation of synapses[28, 29]. Our study indicated that BG45 significantly increased the expression of spinophilin. The staining of the cytoskeletal protein F-actin demonstrated that neurites were shorter in the APPsw group than the control group, and the expression of F-actin was also significantly decreased. However, after treatment with 15 μM BG45, the neurites was more abundant and longer, and the cytoskeletal damage was repaired. Therefore, we speculate that in the early stage of AD, both synapses and the cytoskeleton are damaged. However, BG45 specifically alleviated synaptic damage by downregulating the expression of HDAC1、HDAC2 and HDAC3, while it played a role in enhancing synaptic plasticity.

It has been pointed out that nucleation dependent polymerization takes place in Aβ deposition. When an Aβ oligomer is produced, it triggers the first nucleation step of Aβ deposition and accelerates deposition. At the later stage of Aβ aggregation, Aβ fibrils play an important role, and the role of the Aβ oligomer gradually decreases[30, 31]. Soluble Aβ was only detected in APP/Ps1 transgenic mice at 2.5 and 3.5 months of age[32], while senile plaques were detected in the hippocampus of 7-month-old APP/Ps1 mice, as shown by evaluating the specific emission of broad-spectrum blue violet excitation light from amyloid deposits[33].

Therefore, in the present study, 2 and 6 months of age were selected as the time window of administration. In addition, a group that received a double dose (one dose at 2 months and one dose at 6 months of age) was set up to explore the effects of early and repeated administration. We found that among the treatment groups, the expression of caspase3 and MAP2 in the hippocampus of the 6mBG45 group was significantly higher than that of Tg+(2+6)m BG45 group or even the Tg+2m BG45 group, whereas the expression of MAP2 was lower in the Tg+6m BG45 group; this indicated that the neuroprotective effect of administration at 2-months of age was more pronounced than that of administration at 6-months of age, that is, BG45 might exert an effect on early damage in this AD model. Furthermore, observation of the production of Aβ plaques and the phosphorylation of the tau protein confirmed that the Tg+2m BG45 group and the Tg+(2+6)m BG45 group, showed similar effects that might be better than those of the Tg+6m BG45 group. Studies with a prolonged experimental period should be carried out to further determine the long-term effects of BG45 on these traits.

To verify the results of the in vitro experiments, we examined the mechanism by which BG45 protects hippocampal neurons. First, BG45 significantly inhibited the expression of HDAC2, especially in the Tg+(2+6)m BG45 group. Furthermore, the expression of synaptophysin in the Tg+(2+6)m BG45 group was higher than the Tg+2m BG45 and Tg+6m BG45 groups. In the Tg+6m BG45 group, the expression of spinophilin and PSD-95 was significantly higher than that in the other two groups, while the effect in the Tg+(2+6)m BG45 group on the decreased spinophilin expression was larger than that in the Tg+2m BG45 group. Overall, BG45 ameliorated the damage to synapse-related proteins in early AD in APP/Ps1 transgenic mice. This is bringing the phenotype towards a WT phenotype.

HDAC, a key enzyme in histone deacetylation, is mainly located in the nucleus. It has been found that knockout of the HDAC2 gene increases the expression levels of other synapse-related genes, such as glutamate ion receptor alginate subunit 2 (GRIK2), synaptophysin (SYNPR), sodium voltage-gated channel beta subunit (SCN3B)[34]. In addition, some studies used gene chips to identify genetic pathways related to synaptic function that may be activated by HDACIs[15]. In this study, after treatment with HDACIs, the mRNA levels of GRIK2, SCN3B, SYNPR, Grm2 and Grid2IP, most of which are related to the expression of class I HDAC inhibitors, increased significantly compared with those in the Tg group. These results indicate that among the possible gene pathways activated by HDACIs, BG45 upregulated the expression of GRIK2, SYNPR, SCN3B and Grm2 and grid2IP by inhibiting the deacetylation of HDAC2. We found that most of these genes are related to glutamate receptors, and Grm2 is the gene encoding glutamate receptor subunit 2 (GluR2). Among the treatment groups, the mRNA levels of these genes in the Tg+(2+6) mBG45 group were significantly higher than those in the Tg+2m BG45 and Tg+6m BG45 groups. It can be concluded that BG45 can increase the expression of synapse-related genes in the early stage of AD, and the effect was the most obvious in the Tg+(2+6)m BG45 group.

Due to the changes of the synapse-related genes, we focused on the AMPARs which are closely related to synaptic plasticity. AMPARs are ion channel receptors, and composed of four different glutamate receptor subunits (GluRs) 1, 2, 3, and 4. They participate in the regulation of neurotransmitter release, induce and maintain long-term potentiation (LTP) and long-term depression (LTD) events, and participate in the regulation of learning, memory and other activities. Studies have shown that naturally secreted amyloid oligomers can inhibit LTP in the hippocampus *in vivo*[10]. The absolute magnitude of LTP and LTD is usually compared to assess the deficiency in synaptic plasticity associated with AD[35]. Some researchers found that in 1-month-old transgenic mice, the induction threshold of LTP/LTD showed a tendency to increase LTP at the cost of LTD, while in 6-month-old transgenic mice, this phenotype was reversed to promote LTD and reduce LTP expression[36]. It is concluded that in adult AD mice, the expression of LTP/LTD is altered primarily through synaptic recruitment and phosphorylation of AMPAR, thereby regulating developmental synapse plasticity. During LTP in the hippocampus, GluA1 is first recruited to synapses, and then GluA2 is also recruited to replace GluA1. GluA2/3 interacts with GRIP1/2 and PICK1 through its PDZ domain to form large complexes involved in AMPAR transport[37]. GRIP1 can bind with GRASP, which inhibits the targeting and membrane processes of AMPARs, thus affecting synaptic plasticity.

Impaired function of AMPA receptors is associated with early cognitive impairment in AD. Studies have shown that the levels of Glu receptors 1, 2, and 3 are reduced in the hippocampus of AD patients[38], leading to a decrease in dendritic spines and loss of NMDA receptors[39, 40]. Related studies have shown that HDACI-mediated improvement of synaptic function may be associated with changes in AMPA receptor expression[41]. In recent years, a study confirmed the adverse effect of Aβ on AMPARs. It was found that in hippocampal neurons, $A\beta_{1-42}$ oligomers reduced the expression of AMPA receptors on the postsynaptic membrane and reduced the membrane insertion of new AMPARs and the transport and transfer of mitochondria to dendritic spines[42]. Some researchers also found that the Aβ oligomer preferentially affected the AMPARs containing GluA2, which resulted in the loss of AMPARs and dendritic spines on the surface[43]. Moreover, Aβ increased the phosphorylation level of serine 880 (S880) on GluR2 and significantly reduced the number of GluR2 receptors[44].

Based on these findings, we first detected the expression of the AMPA receptor subunit in an AD cell model. The results showed that the contents of GluA1, GluA2 and GluA3 were decreased in the APPsw cell membrane, while BG45 increased the expression of receptors. In the experiments in APP/Ps1 transgenic mice, it was found that BG45 increased the expression of GluR2/3/4 receptors in transgenic mice, and reduced the phosphorylation level of the serine 880 site (S880) on GluR2. In addition, measurement of gene levels in APP/Ps1 transgenic mice showed that the histone deacetylase inhibitor BG45 blocked the effect of HDACs, activated gene transcription, and upregulated the expression levels of the related genes (GRIK2, SCN3B, SYNPR, Grm2, and Grid2IP); moreover, BG45 blocked the decrease in GluR2 receptor expression in the AD model and reduced the phosphorylation level of GluR2 (S880 site). Therefore, the increased expression of GluR2 binding protein (GRIP1/2) increased the binding of GluR2 to form more transporters, which increased the transport of AMPA receptors; and the inhibitory effect of GluR2 phosphorylation at the S880 site on GluR2 and GRIP1/2 binding was also alleviated by BG45-mediated downregulation of GluR2 phosphorylation. Therefore, we suggest that BG45 may improve synaptic plasiticity by regulating AMPA receptors and changing the expression of synapse-associated proteins.

In conclusion, BG45 reduced the protein expression of APP by specifically inhibiting class I HDACs (HDAC1、HDAC2 and HDAC3), and by decreasing tau phosphorylation, upregulating pre- and postsynaptic protein expression and repairing cytoskeletal damage, BG45 may have improved synaptic plasticity in cell and animal models of early AD. The underlying mechanisms might be associated with the upregulation of AMPARs and synapse-related genes, which further increased the expression of related proteins. This can provide a new idea for the drug treatment of AD. Nevertheless, it is necessary to use neurobehavioral tests to demonstrate the improvement of AD learning and memory function with BG45 treatment. Therefore, in the following studies, we will focus on functional synaptic plasticity in the cells and model animals. And gene chips could be used to identify genetic pathways related to synaptic function that may be activated by HDACIs.

Declarations

Conflict of interest

The authors declare no conflict of interest.

Author contributions

Haiying Ma conceived and designed the experiments. Le Chen, Ying Han and Chunyang Wang performed the experiments. Haiying Ma contributed reagents/materials. Le Chen, Ying Han and Haiying Ma wrote the paper. All the authors are responsible for the data reported and all of them participated in the discussion on the manuscript.

Availability of data and materials

The datasets are available from the corresponding author on reasonable request.

Consent to participate

Not applicable

Consent to publish

Not applicable

Ethics statement

The animal study was reviewed and approved by Institutional Animal Care and Use Committee of the Dalian Medical University in Dalian, China.

Acknowledgments

Not applicable

Funding

This work was supported by the Natural Science Foundation of Liaoning Province [No.20180550468], the Basic Science Foundation of Liaoning Province [No.LJKZ0830] and the Liaoning Provincial Program for Top Discipline of Basic Medical Sciences.

References

1. Lane, C.A., J. Hardy, and J.M. Schott, *Alzheimer's disease.* Eur J Neurol, 2018. **25**(1): p. 59-70.
2. Kowalska, A., *The beta-amyloid cascade hypothesis: a sequence of events leading to neurodegeneration in Alzheimer's disease.* Neurologia I Neurochirurgia Polska, 2004. **38**(5): p. 405-411.

3. Thal, D.R., et al., *Neuropathology and biochemistry of Aβ and its aggregates in Alzheimer's disease.* Acta Neuropathologica, 2015. **129**(2): p. 167-182.
4. Katzmarski, N., et al., *Aβ oligomers trigger and accelerate Aβ seeding.* Brain Pathology, 2019. **30**(1): p. 36-45.
5. De Felice, F.G., et al., *Alzheimer's disease-type neuronal tau hyperphosphorylation induced by Aβ oligomers.* Neurobiology of Aging, 2008. **29**(9): p. 1334-1347.
6. Hillen, H., *The Beta Amyloid Dysfunction (BAD) Hypothesis for Alzheimer's Disease.* Front Neurosci, 2019. **13**: p. 1154.
7. Crimins, J.L., et al., *The intersection of amyloid beta and tau in glutamatergic synaptic dysfunction and collapse in Alzheimer's disease.* Ageing Res Rev, 2013. **12**(3): p. 757-63.
8. Doody, R.S., et al., *Phase 3 trials of solanezumab for mild-to-moderate Alzheimer's disease.* N Engl J Med, 2014. **370**(4): p. 311-21.
9. Lyon, J., *Alzheimer Outlook Far From Bleak.* JAMA The Journal of the American Medical Association, 2017. **317**(9): p. 896.
10. Townsend, M., et al., *Effects of secreted oligomers of amyloid beta-protein on hippocampal synaptic plasticity: a potent role for trimers.* J Physiol, 2006. **572**(Pt 2): p. 477-492.
11. Julie A Harris 1, N.D., Laure Verret, , *Memory retrieval by activating engram cells in mouse models of early Alzheimer's disease.* Neuron, 2010. **68**(3): p. 428-441.
12. Francis, Y.I., et al., *Dysregulation of histone acetylation in the APP/PS1 mouse model of Alzheimer's disease.* J Alzheimers Dis, 2009. **18**(1): p. 131-9.
13. Ishizuka, Y., et al., *Histone deacetylase mediates the decrease in drebrin cluster density induced by amyloid beta oligomers.* Neurochem Int, 2014. **76**: p. 114-21.
14. Singh, P. and M.K. Thakur, *Histone Deacetylase 2 Inhibition Attenuates Downregulation of Hippocampal Plasticity Gene Expression during Aging.* Mol Neurobiol, 2018. **55**(3): p. 2432-2442.
15. Rumbaugh, G., et al., *Pharmacological Selectivity Within Class I Histone Deacetylases Predicts Effects on Synaptic Function and Memory Rescue.* Neuropsychopharmacology, 2015. **40**(10): p. 2307-16.
16. Janczura KJ, V.C., Sartor GC, et al. , *Inhibition of HDAC3 reverses Alzheimer's disease-related pathologies in vitro and in the 3xTg-AD mouse model.* Proceedings of the National Academy of Sciences of the United States of America 2018. **115,47**: p. E11148–E11157.
17. Kilgore, M., et al., *Inhibitors of Class 1 Histone Deacetylases Reverse Contextual Memory Deficits in a Mouse Model of Alzheimer's Disease.* Neuropsychopharmacology, 2009. **35**(4): p. 870-880.
18. Zhu X, W.S., Yu L, et al. , *HDAC3 negatively regulates spatial memory in a mouse model of Alzheimer's disease.* Aging Cell., 2017. **16**(5): p. 1073-1082. .
19. Lovell, M.A., et al., *Elevated thiobarbituric acid-reactive substances and antioxidant enzyme activity in the brain in Alzheimer's disease.* Neurology, 1995. **45**(8): p. 1594-1601.

20. Barnham, K.J., C.L. Masters, and A.I. Bush, *Neurodegenerative diseases and oxidative stress.* Biomedicine & Pharmacotherapy, 2004. **58**(1): p. 39-46.
21. Kong, J.J., et al., *Nicorandil inhibits oxidative stress and amyloid-β precursor protein processing in SH-SY5Y cells overexpressing APPsw.* International Journal of Clinical & Experimental Medicine, 2015. **8**(2): p. 1966-1975.
22. Han, Y., et al., *Class I HDAC Inhibitor Improves Synaptic Proteins and Repairs Cytoskeleton Through Regulating Synapse-Related Genes In vitro and In vivo.* Frontiers in Aging Neuroscience, 2021. **12**.
23. Guan, J.S., et al., *HDAC2 negatively regulates memory formation and synaptic plasticity.* Nature, 2015. **459**(7243): p. 55-60.
24. Ganai, et al., *Modulating epigenetic HAT activity for reinstating acetylation homeostasis: A promising therapeutic strategy for neurological disorders.* Pharmacology & Therapeutics, 2016. **166**: p. 106-122.
25. Zhu, X., Wang, S. , Yu, L. , Jin, J. , Ye, X. , & Liu, Y. , et al., *Hdac3 negatively regulates spatial memory in a mouse model of alzheimer's disease. .* Aging Cell., 2017. **16**: p. 9.
26. Sinclair, L.I., H.M. Tayler, and S.J.N.A.N. Love, *Synaptic protein levels altered in vascular dementia.***41**(4): p. 533-543.
27. Tada, T. and M. Sheng, *Molecular mechanisms of dendritic spine morphogenesis.* Current Opinion in Neurobiology, 2006. **16**(1): p. 95-101.
28. Futter, M., et al., *Phosphorylation of spinophilin by ERK and cyclin-dependent PK 5 (Cdk5).* Proceedings of the National Academy of ences, 2005. **102**(9): p. 3489-3494.
29. Stacie, et al., *Spinophilin is phosphorylated by Ca2+/calmodulin-dependent protein kinase II resulting in regulation of its binding to F-actin.* Journal of Neurochemistry, 2004. **90**(2): p. 317-324.
30. Katzmarski, N., et al., *Abeta oligomers trigger and accelerate Abeta seeding.* Brain Pathol, 2020. **30**(1): p. 36-45.
31. Jeong, S., *Molecular and Cellular Basis of Neurodegeneration in Alzheimer's Disease.* Molecules and Cells, 2017. **40**(9): p. 613-620.
32. Zhang, W., et al., *Early memory deficits precede plaque deposition in APPswe/PS1dE9 mice: involvement of oxidative stress and cholinergic dysfunction.* Free Radic Biol Med, 2012. **52**(8): p. 1443-52.
33. Gao, Y., et al., *Imaging and Spectral Characteristics of Amyloid Plaque Autofluorescence in Brain Slices from the APP/PS1 Mouse Model of Alzheimer's Disease.* Neurosci Bull, 2019. **35**(6): p. 1126-1137.
34. Yamakawa, H., et al., *The Transcription Factor Sp3 Cooperates with HDAC2 to Regulate Synaptic Function and Plasticity in Neurons.* Cell Rep, 2017. **20**(6): p. 1319-1334.
35. Marchetti, C. and H. Marie, *Hippocampal synaptic plasticity in Alzheimer's disease: what have we learned so far from transgenic models?* Rev Neurosci, 2011. **22**(4): p. 373-402.
36. Megill, A., et al., *Defective Age-Dependent Metaplasticity in a Mouse Model of Alzheimer\"s Disease.* Journal of Neuroscience, 2015. **35**(32): p. 11346-11357.

37. Diering, G.H. and R.L. Huganir, *The AMPA Receptor Code of Synaptic Plasticity.* Neuron, 2018. **100**(2): p. 314-329.
38. Yasuda, R.P., et al., *Reduction of AMPA-selective glutamate receptor subunits in the entorhinal cortex of patients with Alzheimer's disease pathology: a biochemical study.* Brain Research, 1995. **678**(1): p. 161-167.
39. Hanley, J.G., *AMPA receptor trafficking pathways and links to dendritic spine morphogenesis.* Cell Adhesion & Migration, 2008. **2**(4): p. 276-282.
40. Iwatsubo, T., et al., *AMPAR removal underlies Abeta-induced synaptic depression and dendritic spine loss.* 2006. **52**(5): p. 831-843.
41. Hsieh, H., et al., *AMPAR removal underlies Abeta-induced synaptic depression and dendritic spine loss.* Neuron, 2006. **52**(5): p. 831.
42. Rui, Y., et al., *Inhibition of AMPA receptor trafficking at hippocampal synapses by β-amyloid oligomers: the mitochondrial contribution.* Molecular Brain, 2010. **3**(1): p. 1-13.
43. Zhao, W.Q., et al., *Inhibition of Calcineurin-mediated Endocytosis and α-Amino-3-hydroxy-5-methyl-4-isoxazolepropionic Acid (AMPA) Receptors Prevents Amyloid β Oligomer-induced Synaptic Disruption.* Journal of Biological Chemistry, 2010. **285**(10): p. 7619-7632.
44. Liu, S.-J., et al., *Amyloid-β Decreases Cell-Surface AMPA Receptors by Increasing Intracellular Calcium and Phosphorylation of GluR2.* Journal of Alzheimer's Disease, 2010. **21**(2): p. 655-666.

Figures

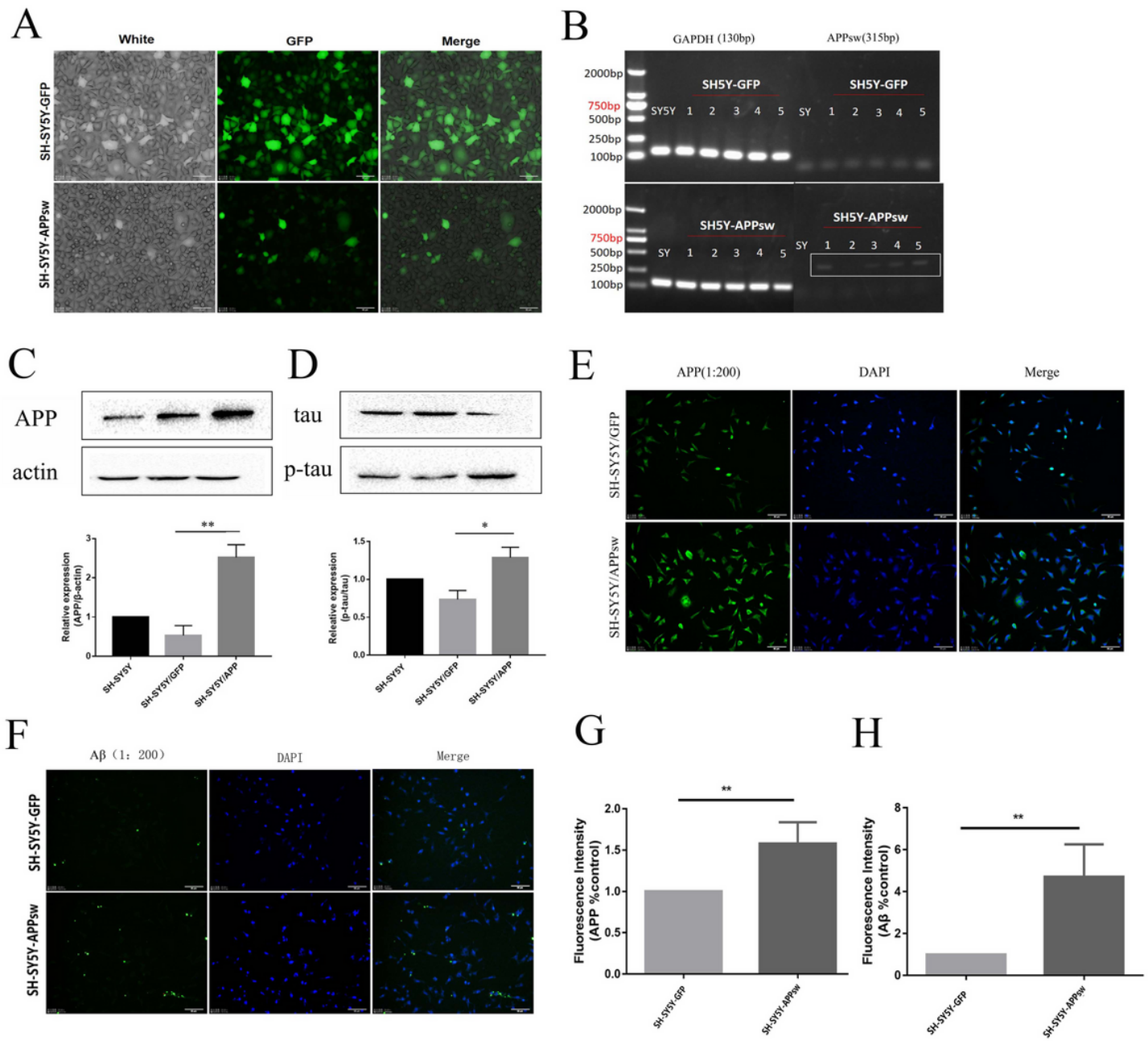

Figure 1

SH-SY5Y cells transfected with the APPsw gene were established as an AD cell model. A) Transfection efficiency was observed in the SH-SY5Y cell. B) The expression of the APPsw gene was detected in different SH-SY5Y cell clones by RT-PCR. C) Immunoblot analysis of APP in GFP and APPsw cells. Quantification of APP normalized to β-actin and expressed as a % of control showed significant differences between SH-SY5Y cells and APPsw cells ($p<0.01$). D) Immunoblot analysis of tau and p-tau in GFP and APPsw cells. Quantification of p-tau normalized to tau and expressed as a % of control showed significant differences between SH-SY5Y cells and APPsw cells ($p<0.05$). E&G) Immunofluorescence staining analysis of APP in GFP and APPsw cells ($p<0.05$). F&H) Immunofluorescence staining analysis

of Aβ in GFP and APP cells ($p<0.05$). All values are presented as the mean ± SD from three experiments. n=5. *$p<0.05$, **$p<0.01$, ***$p<0.001$.

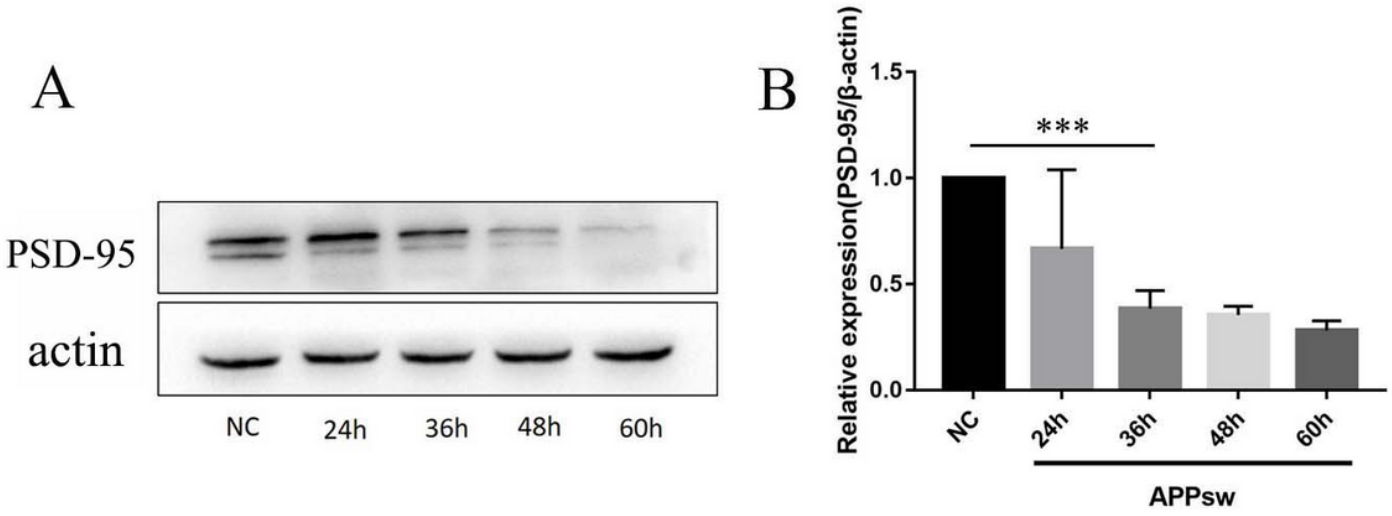

Figure 2

The expression of PSD-95 in APPsw cells at different times. A) Immunoblot analysis of PSD-95 from SH-SY5Y cell at 60 h and APPsw cells at different times (24 h, 36 h, 48 h and 60 h). B) Quantification of PSD-95 normalized to β-actin and expressed as a % of control showed significant differences between SH-SY5Y cells and APPsw cells at 36 h ($p<0.001$). All values are presented as the mean ± SD from three independent experiments. n=5. *$p<0.05$, **$p<0.01$, ***$p<0.001$.

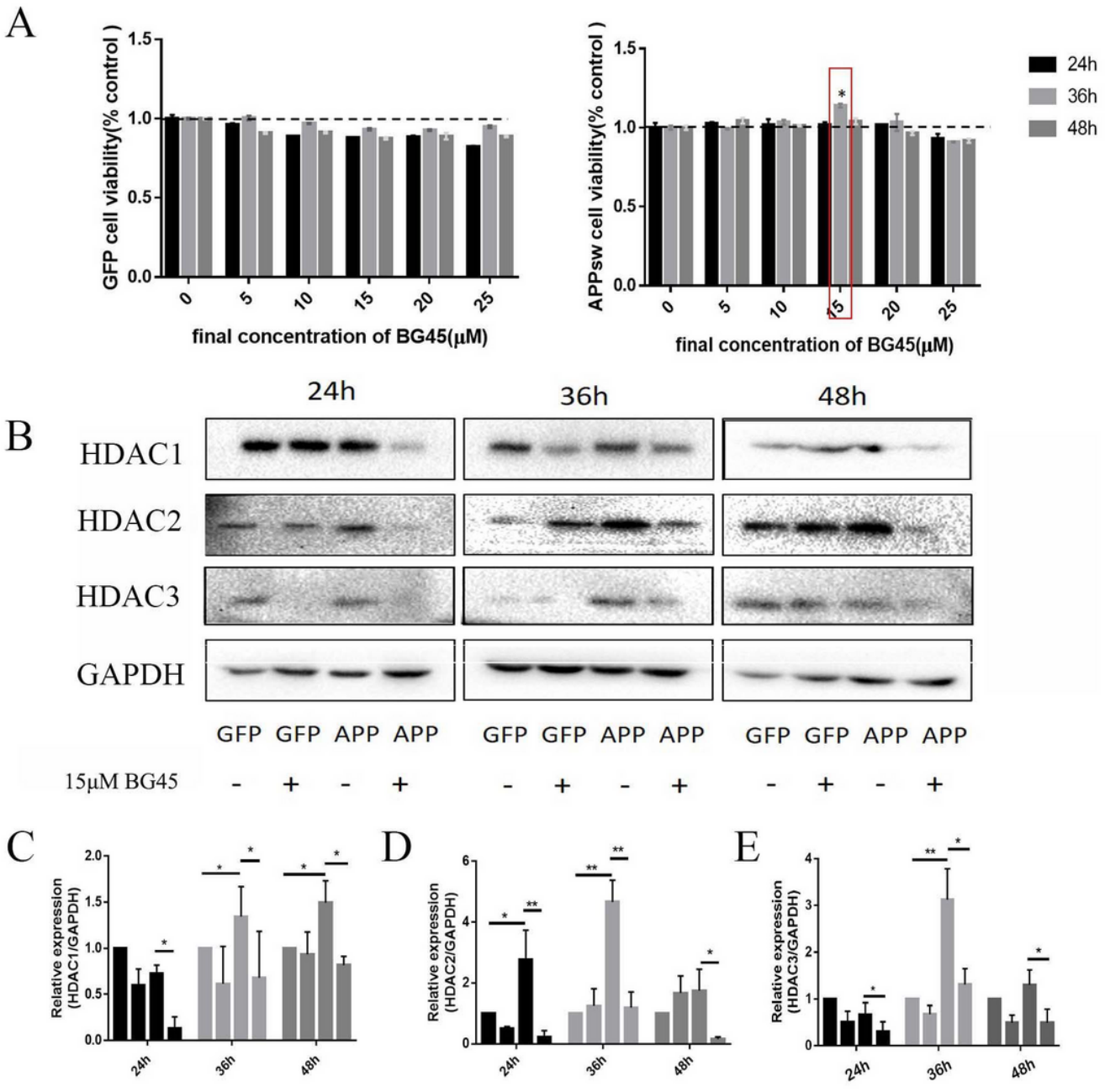

Figure 3

The effects of BG45 on class I HDACs (HDAC1, 2, and 3). A) The effect of BG45 on GFP and APPsw cell viability. B) Immunoblot analysis of HDAC1, 2, and 3 in GFP and APPsw cells treated with vehicle or BG45 (15 μM) for different amounts of time. C) Quantification of HDAC1 analysis. D) Quantification of HDAC2 analysis. E) Quantification of HDAC3 analysis. All values are presented as the mean ± SD from three independent experiments. n=5. *p<0.05, **p<0.01, ***p<0.001.

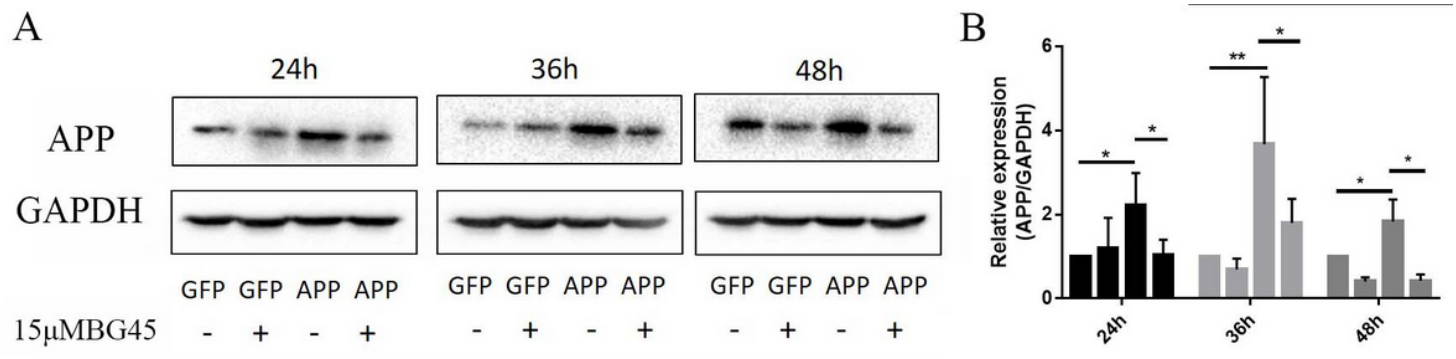

Figure 4

Effects of BG45 on APP proteins. A) Immunoblot analysis of APP in GFP and APPsw cells treated with vehicle or BG45 (15 μM). B) Quantification of APP analysis. All values are presented as the mean ± SD from three independent experiments. n=5. *p<0.05, **p<0.01, ***p<0.001.

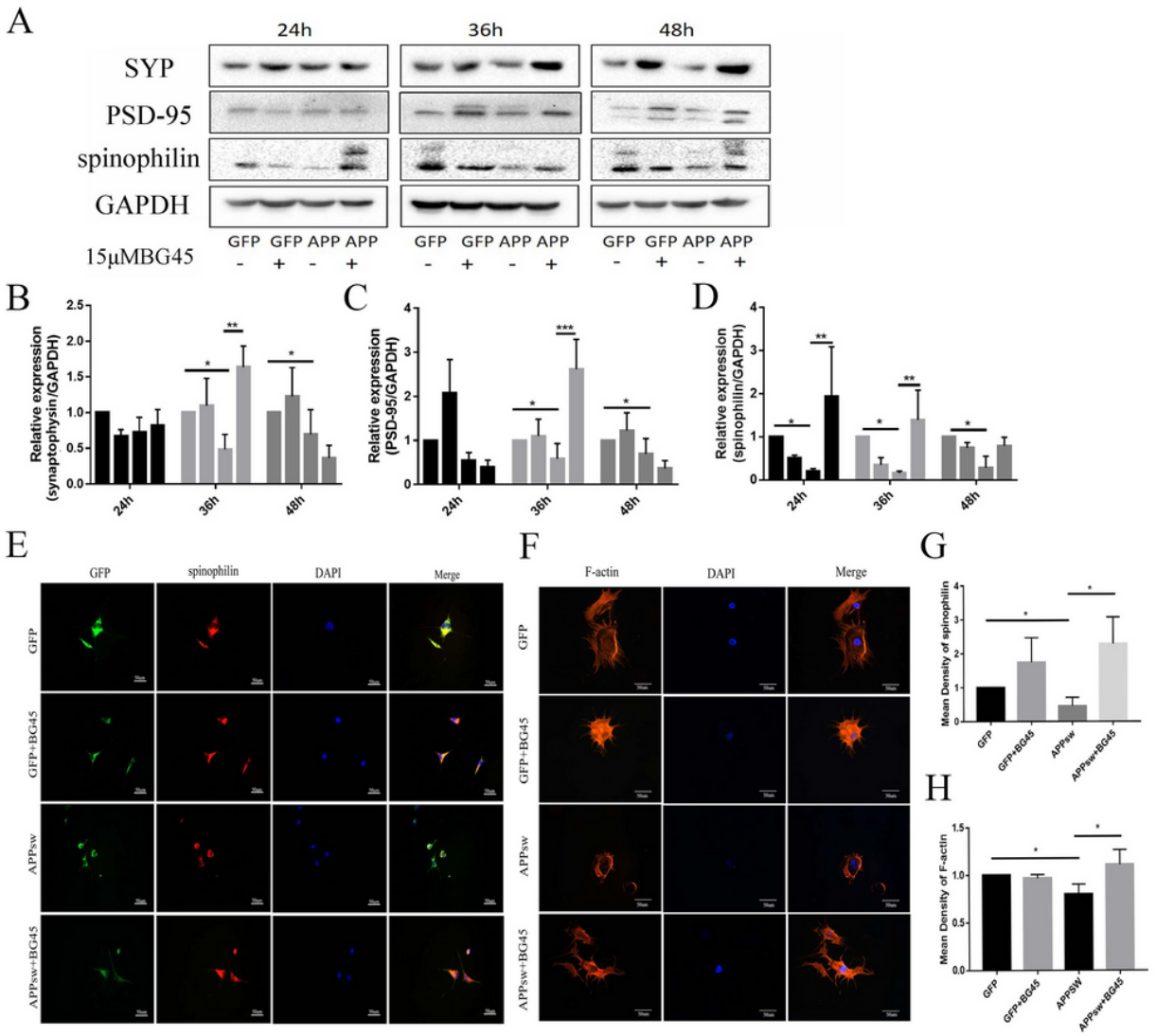

Figure 5

The effects of BG45 on synapse-related proteins and F-actin. A) Immunoblot analysis of SYP, PSD-95 and spinophilin in GFP and APPsw cells treated with vehicle or BG45 (15 μM) for different times (24 h, 36 h and 48 h). B) Quantification of SYP analysis. C) Quantification of PSD-95analysis. D) Quantification of spinophilin analysis. E) Immunofluorescence staining analysis of spinophilin in GFP and APPsw cells treated with vehicle or BG45 (15 μM) for 36 h. F) Immunofluorescence staining analysis of phalloidin/F-actin in GFP and APPsw cells treated with vehicle or BG45 (15 μM) for 36 h. G) Quantification of spinophilin analysis. H) Quantification of F-actin analysis. All values are presented as the mean ± SD from three independent experiments. n=5. *p<0.05, **p<0.01, ***p<0.001.

Figure 6

BG45 increased the cell surface levels of AMPA receptor subunits. A) Immunostaining analysis of cell surface GluA1, GluA2 and GluA3 receptors on GFP and APPsw cells treated with vehicle or BG45 (15 μM). The lower images are the positive cells magnified in the white box. B) Quantification of the surface GluA1 data. C) Quantification of the surface GluA2 data. D) Quantification of the surface GluA3 data. All values are presented as the mean ± SD from three independent experiments. n=5. *p<0.05, **p<0.01, ***p<0.001.

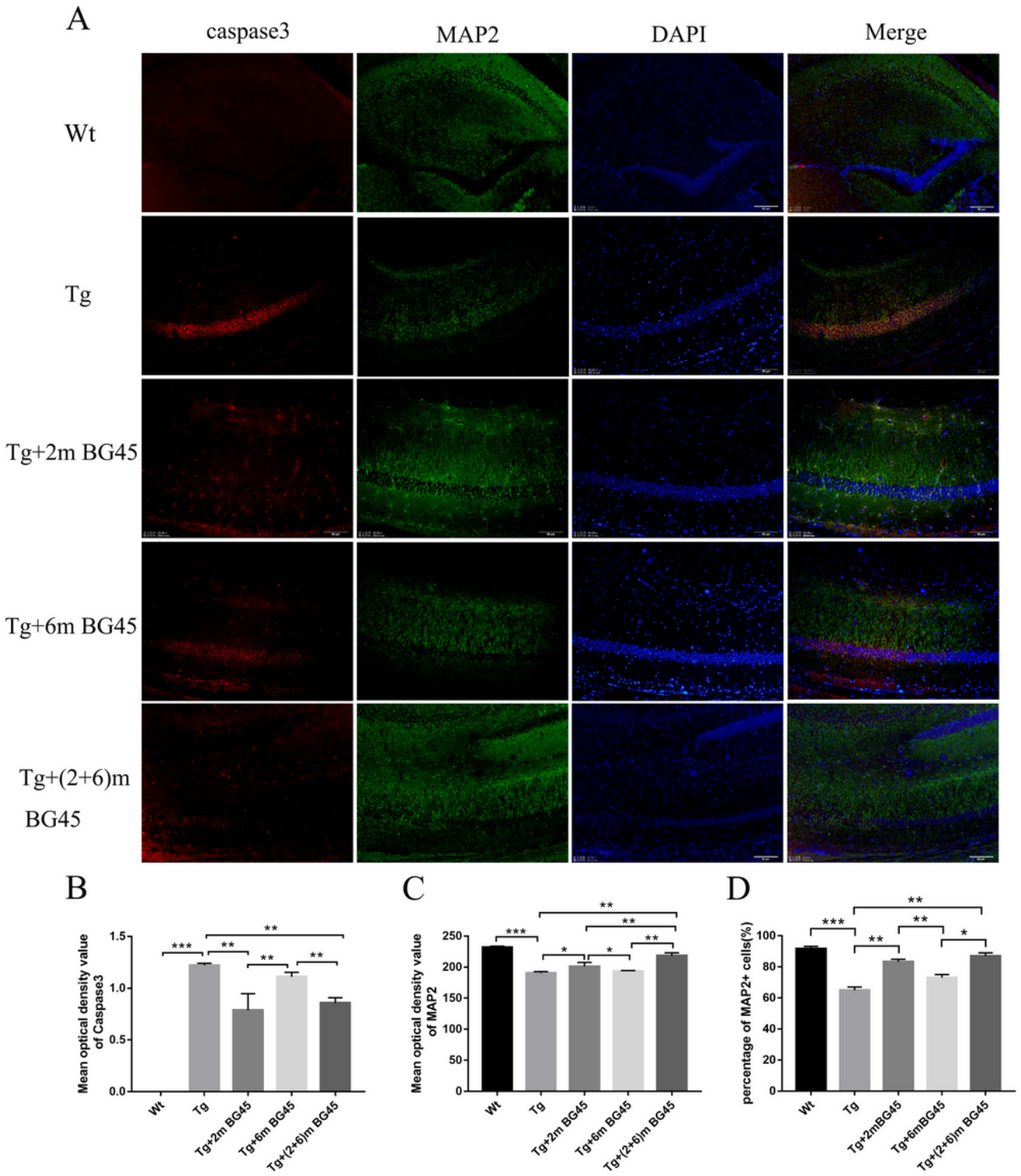

Figure 7

Protective effect of BG45 on hippocampal neurons in APP/Ps1 transgenic mice. A) Immunofluorescence analysis of the caspase3 and MAP2 proteins in hippocampal neurons treated with vehicle or BG45. B) Quantification of the caspase3 protein data. C) Quantification of the MAP2 protein data. D) Percentage of MAP2+ cells. All values are presented as the mean ± SD from three independent experiments. n=5. *p<0.05, **p<0.01, ***p<0.001.

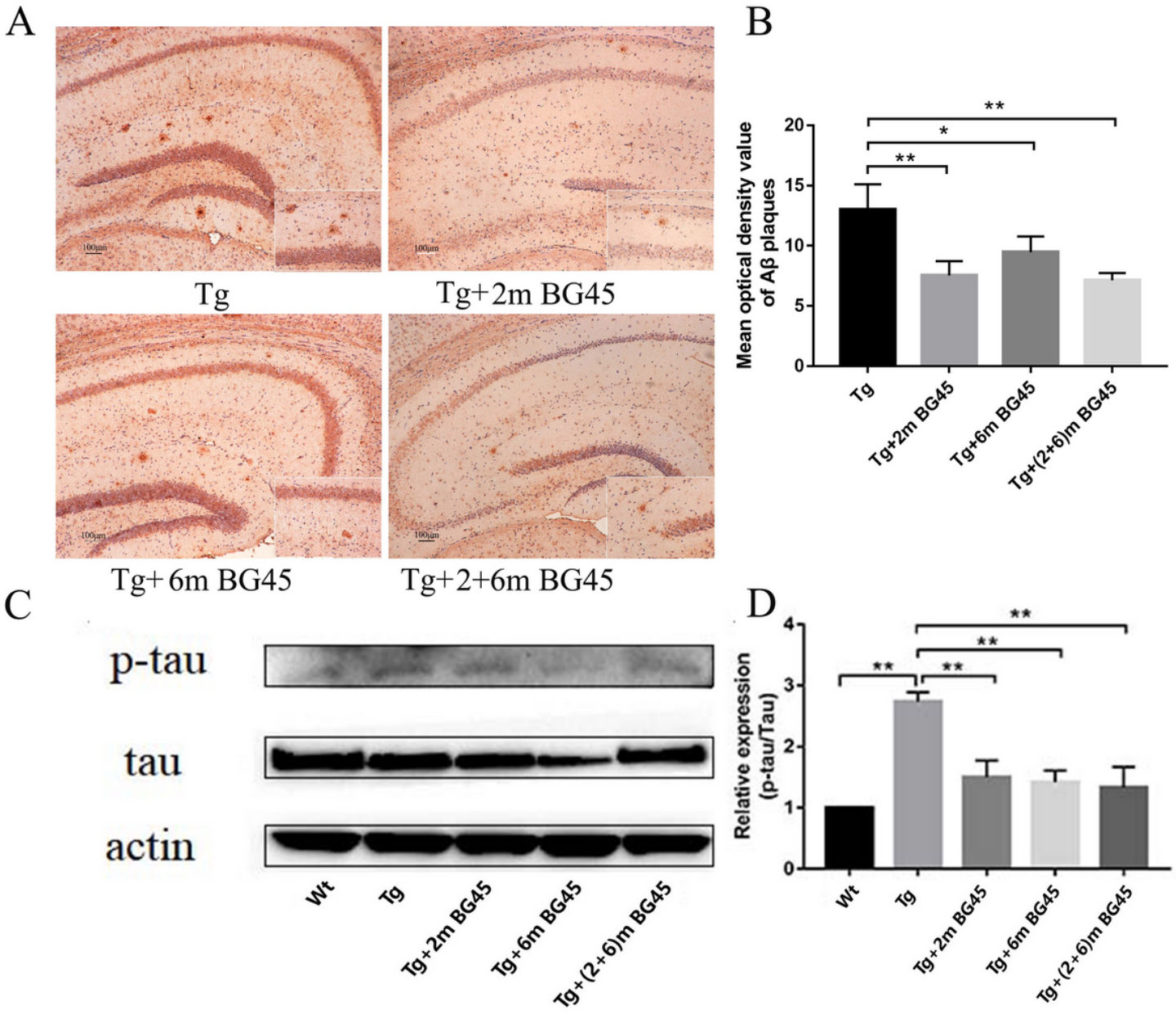

Figure 8

BG45 decreased the Aβ deposition of hippocampal neurons and the phosphorylation level of the tau protein in APP/Ps1 transgenic mice. A) Immunohistochemistry of Aβ deposition in hippocampal neurons treated with vehicle or BG45. In the lower right corner of the image is the magnified part to show Aβ deposition clearly. B) Quantification of the Aβ deposition data. C) Western blot of the protein expression of p-tau/tau in hippocampal neurons treated with vehicle or BG45. D) Quantification of the tau protein phosphorylation level data. All values are presented as the mean ± SD from three independent experiments. n=5. *p<0.05, **p<0.01, ***p<0.001.

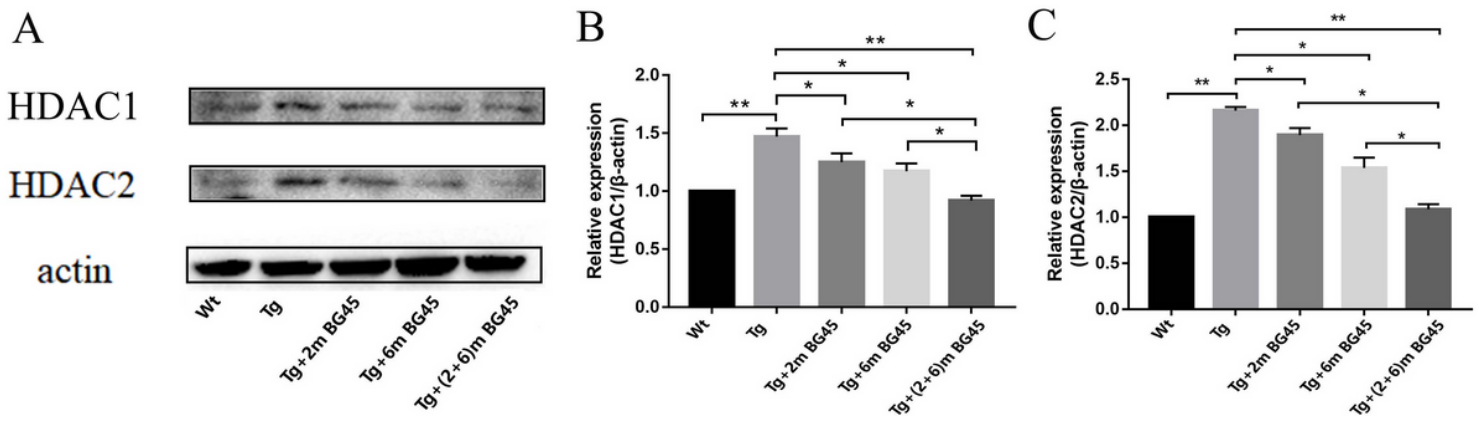

Figure 9

BG45 reduced HDAC1 and HDAC2 protein expression in the hippocampal neurons of APP/Ps1 mice. A) Immunoblot analysis of the HDAC1 and HDAC2 proteins in the hippocampus treated with vehicle or BG45. B) Quantification of the HDAC1 data. C) Quantification of the HDAC2 data. All values are presented as the mean ± SD from three independent experiments. n=5. *p<0.05, **p<0.01, ***p<0.001.

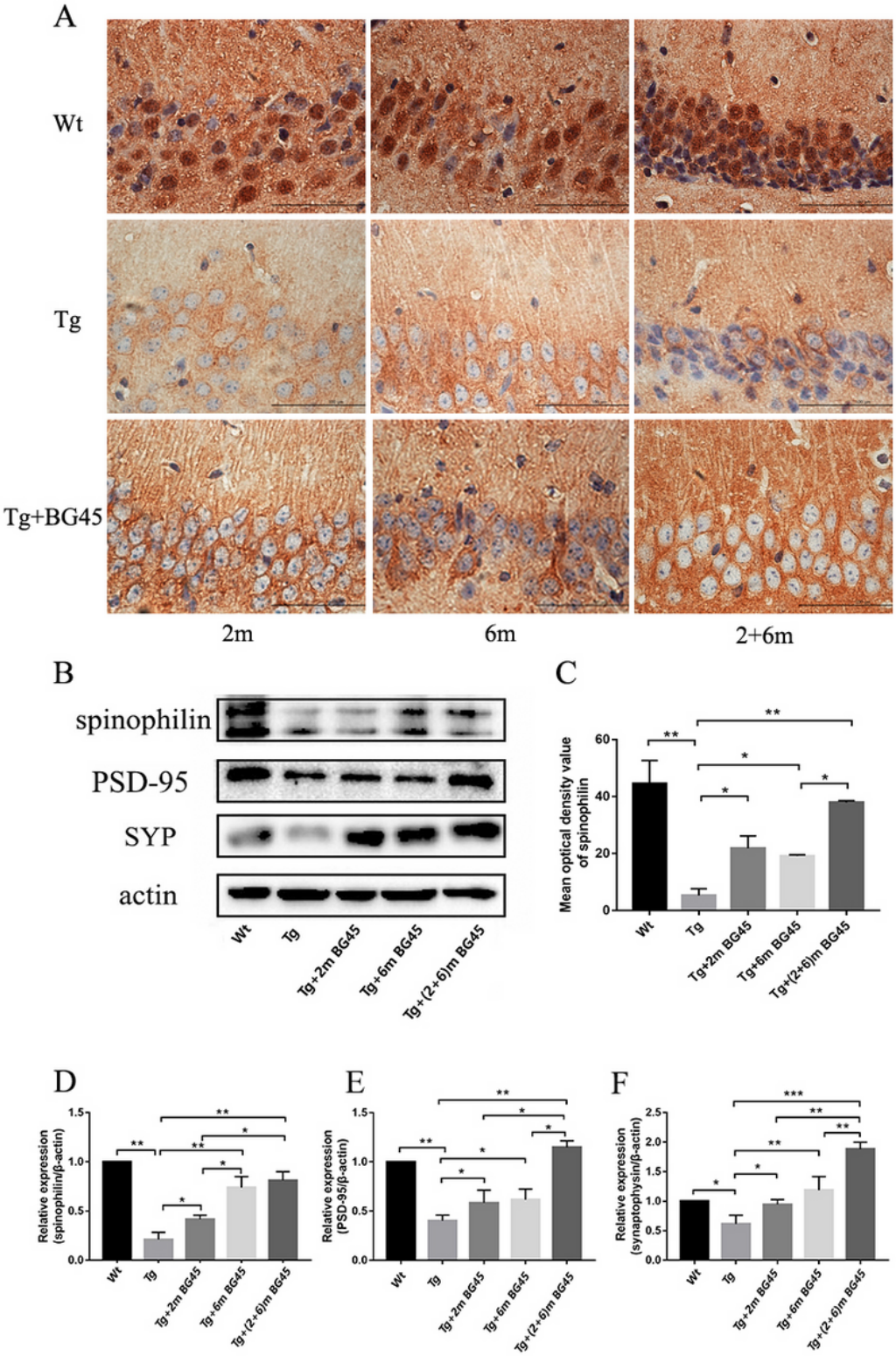

Figure 10

BG45 upregulates the expression of synaptic-related proteins in hippocampal neurons of APP/Ps1 mice. A) Immunohistochemistry of spinophilin protein in hippocampal neurons treated with vehicle or BG45. B) Immunoblot analysis of spinophilin、PSD-95 and synaptophysin protein in the hippocampus treated with vehicle or BG45. C) Quantification of spinophilin data in the hippocampus. D)-F) Quantification of data

from synapse-related proteins. All values are presented as the mean ± SD from three independent experiments. n=5. *p<0.05, **p<0.01, ***p<0.001.

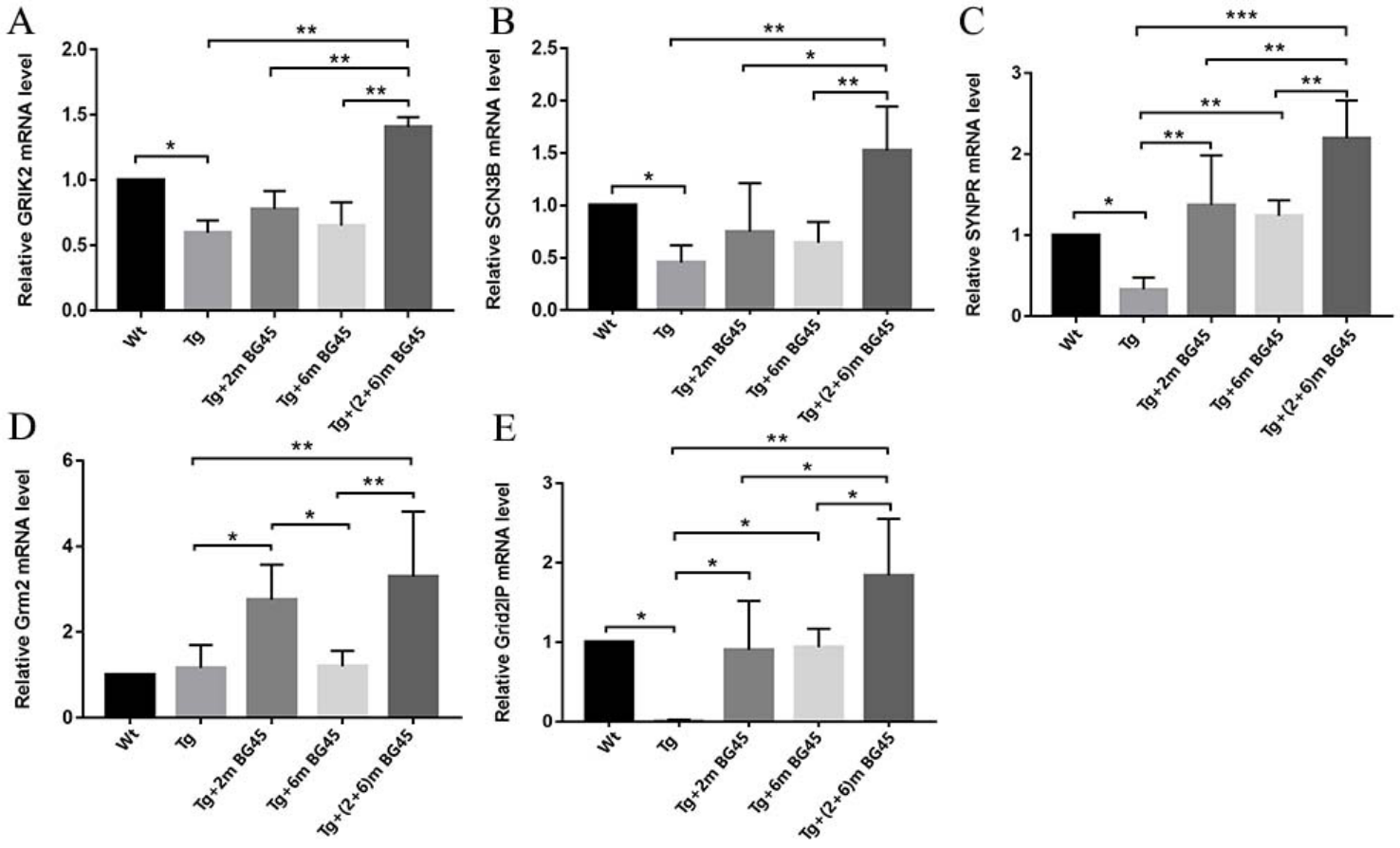

Figure 11

BG45 increased the levels of synapse-related genes (GRIK2, SCN3B, SYNPR, Grm2 and Grid2IP) in APP/Ps1 mice. A)-E). The mRNA expression levels of GRIK2, SCN3B, SYNPR, Grm2 and Grid2IP. All values are presented as the mean ± SD from three independent experiments. n=5. *p<0.05, **p<0.01, ***p<0.001.

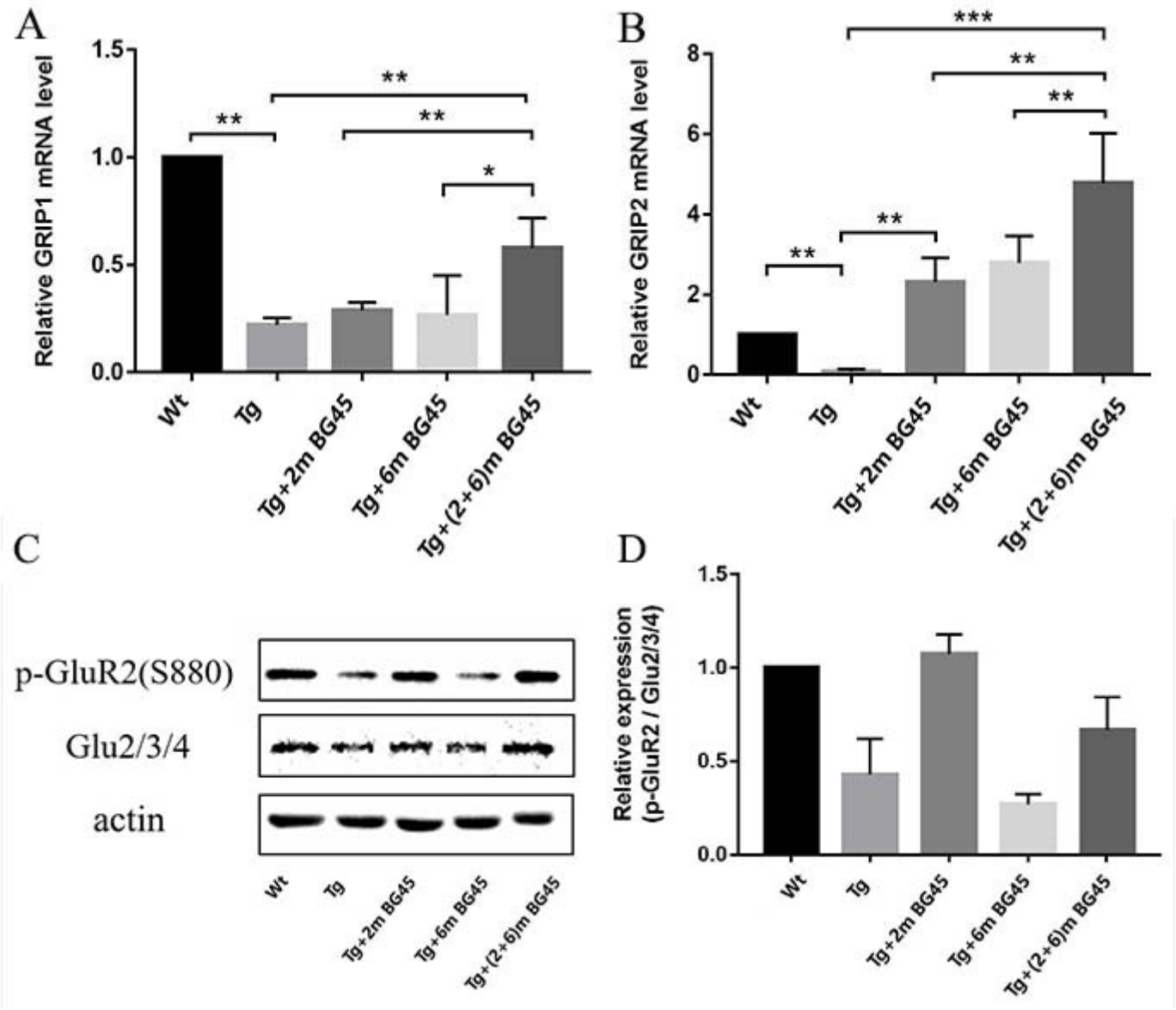

Figure 12

Effects of BG45 on the expression level of glutamate receptor protein and related genes. A)-B). The mRNA expression levels of GRIP1 and GRIP2. C) Immunoblot analysis of p-GluR2 (s880) and Glu2/3/4 in the hippocampus treated with vehicle or BG45. D) Quantification of p-GluR2 data in the hippocampus. All values are presented as the mean ± SD from three independent experiments. n=5. *p<0.05, **p<0.01, ***p<0.001.